SI Appendix

Supplementary Methods

Molecular Biology:

For expression in neurons, the iC1C2 (1) gene was cloned into an AAV vector plasmid between AgeI and NotI sites. The gene was expressed under the CamKIIα promotor unless otherwise noted and fused to eYFP via a linker region containing the TS (2) sequence for improved membrane trafficking and expression. For HEK cell expression, human codon-adapted iC1C2 (1) gene was cloned into p-EGFP-C1 vector using NheI and AgeI restriction sites. EGFP was replaced by mCherry using AgeI and XhoI restriction sites. Point mutations were introduced using QuikChange mutagenesis (Agilent Technologies, Santa Clara, CA, USA), no TS sequence was used.

Figures of protein structures were prepared using PyMOL Molecular Graphics System, Version 1.7.0.1 (Schrödinger, LLC). Replacement of residues in the C1C2 structure (Protein data base number: 3UG9) were conducted with Pymol 1.7.0.1. Electrostatic potentials were calculated using Pymol's APBS Tool 2.1 (3), and were obtained at an ionic strength of 150 mM. The dielectric constants were 2 for the protein and 78 for the solvent.

Neuronal culture preparation:

Hippocampal neurons: Primary cultured hippocampal neurons were prepared as described previously (1). The hippocampi was removed from Spague-Dawley rat pups (Charles River) at postnatal day 0 (P0). The CA1 and CA3 regions were digested with 0.4 mg/mL papain (Worthington), and plated onto 12 mm glass coverslips pre-coated with 1:30 Matrigel (Beckton Dickinson Labware). Cells were plated at a density of 65,000 cells per well in 24-well plates. The cultures were maintained in Neurobasal-A medium (Invitrogen) containing 1.25% FBS (HyClone), 4% B-27 supplement (Gibco), 2 mM Glutamax (Gibco) and 2 mg/ml fluorodeoxyuridine (FUDR, Sigma), and maintained in a humid culture incubator with 5% CO_2 at 37°C.

Cells were transfected 6-10 days *in vitro* (DIV). For each well to be transfected, a DNA-$CaCl_2$ mix containing the following was prepared: 2 µg of DNA (prepared using an endotoxin-free preparation kit (Qiagen)) 1.875 µl 2M $CaCl_2$, and sterile water to a total volume of 15 µl. An additional 15 µl of 2X filtered HEPES-buffered saline (HBS, in mM: 50 HEPES, 1.5 Na_2HPO_4, 280 NaCl, pH 7.05 with NaOH) was added per DNA-$CaCl_2$ mix, and then incubated at room temperature for 20 minutes. In the meantime, the neuronal growth medium was removed from the wells and kept at 37°C, and replaced with 400 µl pre-warmed minimal essential medium (MEM). After incubation of the DNA-$CaCl_2$-HBS mix was complete, it was added dropwise into each well, and the plates were transferred to the culture incubator for 45-60 minutes. Each well was then washed three times with 1 ml of MEM (pre-warmed to 37°C), after which the MEM was replaced with the original neuronal growth medium. The plates were placed in the culture incubator and kept until recordings were performed.

DRG neurons: Isolation of DRGs: DRG excision, culture and electrophysiology procedures were largely based on previously reported protocols (4). Mice, three weeks after

intraneural injection, were deeply anesthetized with isofluorane 5%. Mice were then perfused with 4°C sterile phosphate buffered saline. The following isolation steps were rapidly performed, and completed within 7 minutes after perfusion. After removing the skin from the back, using sterile procedure, the muscles along the vertebral column were cut and bone rongeurs used to peel away any muscle or tendon superficial to the vertebrae. The rongeurs were used to break away the vertebral bone directly dorsal to the spinal cord, starting at the base of the spine, and moving rostrally. Muscle lateral to the spinal cord was peeled away until the sciatic nerve branches could be visualized, and bones were broken lateral to the spinal cord to free the path of the nerve. Each nerve branch was cut using small spring scissors and pulled proximally with forceps until the dorsal root ganglion could be visualized, and cut proximal to the DRG. The DRG was then placed in 4°C, sterile MEM-complete solution (minimal essential media, MEM vitamins, antibiotics, and 10% fetal bovine serum). Two to three DRG were excised from each expressing side of the mouse.

Culturing of DRGs: Excised DRGs were desheathed and transferred to MEM-Collagenase solution (minimal essential media, vitamins, antibiotics, no fetal bovine serum, 0.125% collagenase). The tissue was incubated at 37°C for 45 minutes in a water bath and then triturated in 2.5 ml TripleE Express (Invitrogen). The trypsin was quenched with 2.5 ml MEM-complete with 80 ug/ml DNase I, 100 ug/ml trypsin inhibitor from chicken egg white and 2.5mg/ml $MgSO_4$. Cells were centrifuged, and resuspended in trypsin-free MEM-complete at a cell density of 500,000 cells/m,l. 100 ul of the cell suspension was carefully placed as a bubble on Matrigel-coated coverslips, and then incubated at 37°C, 3% CO2, 90% humidity. Two hours after initial incubation, the cultured neurons were flooded with 1 ml of MEM-complete. Cells were maintained 2-7 days in culture with fresh media changes as needed until electrophysiology was performed.

Stereotactic virus injection and animals for patch clamp recordings:

pAAV-CaMKIIa-iC++-TS-eYFP, pAAV-EF1a-DIO-iC++-TS-eYFP, and pAAV-CaMKIIa-SwiChR++-TS-eYFP were packaged as AAV8/Y733F at the Stanford Neuroscience Gene Vector and Virus Core.

4-6 week old mice were sterotactically injected with 1 µl virus, with titers matched at 1.5e12 vg/ml for the iC++ viruses and set at 7.5e12 vg/ml for the SwiChR++ virus. The CaMKIIα-driven viruses were used for expressing opsin in mPFC pyramidal cells of wild-type animals (male, C57BL/6J). The Cre-dependent DIO viruses were used for expressing opsins in hippocampal PV+ interneurons using PValb::Cre transgenic mice (5) (male and female) (Jackson Laboratory stock #: 008069) and in substantia nigra dopaminergic neurons using DAT::Cre transgenic mice (6) (male and female) (Jackson Laboratory stock #: 006660). Injections were made at the following coordinates (from bregma) for the various brain regions: mPFC: AP +1.7 mm, ML +0.3 mm, DV -2.5 mm; hippocampus: AP -2.2 mm, ML +1.75 mm, DV -1.4 mm and AP -2.3 mm, ML +2.0 mm, DV -1.3 mm; substantia nigra: AP: -3.0 mm, ML: +/- 1.1 mm, DV: -4.08 mm.

Intrasciatic injection in wild-type mice (female, C57BL/6) was performed as previously described for DRG neurons (4). Briefly, under anesthesia, the sciatic nerve was exposed, freed of the underlying fascia, and injected with 5 ul (7 x 10^10 vg) of AAV6-hSyn-iC++-TS-eYFP (2.5 ul in each fascicle).

Buprenex was applied after the surgery. We monitor our animals for one hour after the surgery and control if they show normal activity such as grooming and exploring. This procedure is repeated every day after the surgery and then weekly whereas we also control the healing of the surgical incision. Animals were kept under a standard 12 h light/dark cycle and were housed

individually or in groups between 2 and 5 animals. All experiments and procedures are approved by the Stanford Administrative Panel on Laboratory Animal Care which is accredited by the Association for Assessment and Accreditation of Laboratory Animal Care International.

***In vitro* electrophysiology:**

HEK293 Cell Recordings:

HEK293 cells were cultured as described (7), seeded onto coverslips at a concentration of 1.25 x 10^5 cells · ml^{-1} and supplemented with 1 µM *all trans*-retinal. Cells where transiently transfected using Fugene HD (Roche, Mannheim, Germany) 48 h before measurements. Signals were amplified and digitized using AxoPatch200B and DigiData1400 (Molecular Devices, Sunnyvale, CA, USA). A Polychrome V (TILL Photonics, Planegg, Germany) adjusted to 490 ± 7 nm served as light source. Activation light was coupled into an Axiovert 100 microscope (Carl Zeiss, Jena, Germany) and modulated with a programmable shutter system (VS25 and VCM-D1, Vincent Associates, Rochester, NY, USA). Patch pipettes were pulled using a P97 micropipette puller (Sutter Instruments, Novato, CA, USA), followed by fire-polishing resulting in pipette resistances between 1.5 and 2.5 MΩ. All whole-cell recordings had a minimum membrane resistance of 500MΩ (usually >1GΩ) whereas the access resistance was kept below 10MΩ. Liquid junction potentials were corrected online (see below).

Chloride dependent measurements in HEK293 cells: For all experiments external buffer solutions were exchanged by superfusion of at least 4 ml of the respective buffer into the custom made recording chamber (volume ~500 µl) while the fluid level was controlled by MPCU bath handler (Lorenz Messgerätebau, Katlenburg-Lindau, Germany). Buffer compositions are listed in table 1. The pH of all buffers was adjusted with N-methyl-D-glucamine or citric acid to pH 7.20. The final osmolarity was adjusted to 320 mOsm for extracellular solutions and 290 mOsm for intracellular solutions.

All experiments were carried out at 25°C. To maintain a stable reference (bath) electrode potential we used a 140mM NaCl agar bridge. Patch clamp recordings where performed under balanced chloride conditions to exclude chloride adulteration. Under these conditions electrodes were compensated to a potential of 0mV. As the change of extracellular chloride concentration causes a liquid junction potential (LJP), all measurements have been corrected on-line for occuring LJP. The values used for LPJ correction were calculated as described elsewere[2] and are listed in table M2. For anion selectivity measurements 140mM NaCl was replaced with 140mM NaX (X= Aspartate, gluconate, bromide, iodide) in the extracellular buffer. The liquid junction potential was therefore corrected for 0, 2.1, 10.8, 10.5mV, respectively.

Table M1: intra- and extracellular buffer composition.

	extracellular [Cl^-]			**intracellular [Cl^-]**		
	10mM	**50mM**	**150mM**	**10mM**	**50mM**	**120mM**
$MgCl_2$	2	2	2	2	2	2
$CaCl_2$	2	2	2	2	2	2
KCl	1	1	1	1	1	1
CsCl	1	1	1	1	1	1
EGTA	-	-	-	10	10	10
HEPES	10	10	10	10	10	10
NaCl	-	40	140	-	40	110
NaASP	140	100	-	110	70	-

Abbreviations used: ethylene glycol tetraacetic acid (EGTA), 4-(2-hydroxyethyl)-1-piperazineethanesulfonic acid (HEPES), Aspartate (ASP). All concentrations in mM.

Table M2: Liquid junction potential correction used for measurements

intracellular [Cl-]	extracellular [Cl-]		
	10mM	**50mM**	**150mM**
10mM	0	1.7	10.5
50mM	-6.9	0	6.4
120mM	-12.6	-8.1	0

All Liquid junction potential corrections are given in mV.

Light intensities – The applied light intensity for conventional current voltage recordings at 490 nm was 2.99 mW/mm², measured after passing through all optics and coverslip with a calibrated optometer (P 9710, Gigahertz Optik, Türkenfeld, Germany). Measured light intensities are given for the illuminated field of the W Plan-Apochromat 40x/1.0 DIC objective (0.264mm²). For wavelength dependent measurements (recording of action spectrum), a motorized neutral density filter wheel (NDF) (Newport, Irvine, CA, USA) was inserted into the light path to gain the same photonflux for all wavelengths. A custom software written in Labview (National Instruments, Austin, TX, USA) was used to control the NDF and synchronize it with electrophysiological experiments. Light was applied for 10ms.

Neuronal cultures:

Electrophysiological recordings of cultured neurons were performed 6-8 days after transfection for hippocampal neurons, and 3 days after culture preparation for DRG neurons. All testes opsin constructs were eYFP tagged and contained the trafficking sequence TS[2]. The external recording solution for hippocampal neurons contained (in mM): 147 $[Cl^-]_{ext}$: 135 NaCl, 4 KCl, 10 HEPES, 2 $CaCl_2$, 2 $MgCl_2$, 30 D-glucose, pH 7.3 and for DRG neurons contained (in mM): 132 $[Cl^-]_{ext}$: 123 NaCl, 3 KCl, 26 HEPES, 2 $CaCl_2$, 1 $MgCl_2$, 1.25 NaH_2PO_4 and 11 glucose, pH 7.3 The recording medium also contained the synaptic transmission blockers D-2-amino-5-phosphonovaleric acid (APV; 25 μM), 2,3-dihydroxy-6-nitro-7-sulfamoyl-benzo[f]quinoxaline-2,3-dione (NBQX; 10 μM), and gabazine (10 μM). The internal recording solution contained in mM: 4 $[Cl^-]_{int}$: 140 K-Gluconate, 2 $MgCl_2$, 10 HEPES, 10 EGTA, pH 7.2. 12 $[Cl^-]_{int}$: 131 K-Gluconate, 8 KCl, 2 $MgCl_2$, 10 HEPES, 10 EGTA, pH 7.2. Action potentials were evoked by pulsed electrical current injections at 10 or 20 Hz with either 30 ms pulse widths and current amplitudes at 191 pA ± 10, or 5 ms pulse widths and current injections at 520 pA ± 22. Current injections were individually titrated for each cell and chosen based on minimal amplitudes necessary to reach threshold for action potential generation (V_{AP}). Action potentials were inhibited for 4 seconds by light application. For 10 ms pulsed protocols, electrical current injections were applied for 12 seconds between the minimum necessary to evoke action potentials and the maximum current which could be inhibited during a 10 s light application. Fluorescence measurements were performed by measuring the eYFP fluorescence of individual cells by 512 nm light exposure. The fluorescence intensity and cell size was analyzed using ImageJ (Wayne Rasband, NIH, USA). V_{AP} was measured individually for each cell at the voltage deflection point at which the first-order derivative of the membrane potential (dV/dt) exhibited a sharp transition, typically > 10mV/ms.

Acute slice:

Acute slice recordings were performed at least 4 weeks after injection of the opsin-encoding viruses that also contained tagged eYFP and the TS^2 sequence for improved membrane trafficking. Coronal slices (300 μm) prepared after intracardial perfusion with ice-cold, sucrose-containing artificial cerebrospinal fluid solution (ACSF; in mM): 85 NaCl, 75 sucrose, 2.5 KCl, 25 glucose, 1.25 NaH_2PO_4, 4 $MgCl_2$, 0.5 $CaCl_2$ and 24 $NaHCO_3$. Slices were incubated 1 hour at 32–34 °C, and then were transported to room temperature oxygenated ACSF solution (in mM): 132 $[Cl^-]_{ext}$: 123 NaCl, 3 KCl, 26 $NaHCO_3$, 2 $CaCl_2$, 1 $MgCl_2$, 1.25 NaH_2PO_4 and 11 glucose. The ACSF also contained synaptic transmission blockers D-2-amino-5-phosphonovaleric acid (APV; 25 μM), 2,3-dihydroxy-6-nitro-7-sulfamoyl-benzo[f]quinoxaline-2,3-dione (NBQX; 10 μM), and gabazine (10 μM) for recordings. For the oxytocin experiments, cells were first recorded for 30 seconds to establish the baseline potential, and then TGOT ($[Thr^4,Gly^7]$-oxytocin, 1 μM), a selective agonist for the oxytocin receptor, was bath-applied after baseline. Recording patch pipettes contained the following solution (in mM): 4 $[Cl^-]_{int}$: 140 K-Gluconate, 2 $MgCl_2$, 10 HEPES, 10 EGTA, pH 7.2. 12 $[Cl^-]_{int}$: 131 K-Gluconate, 8 KCl, 2 $MgCl_2$, 10 HEPES, 10 EGTA, pH 7.2. 20 $[Cl^-]_{int}$: 123 K-Gluconate, 16 KCl, 2 $MgCl_2$, 10 HEPES, 10 EGTA, pH 7.2.

In vitro patch clamp recordings:

Liquid junction potentials (4 mM $[Cl^-]_{int}$: -14.4 mV, 12 mM $[Cl^-]_{int}$: -13.6 mV, 20 mM $[Cl^-]_{int}$: -12.8 mV) were corrected for all measurements. Photocurrents and reversal potentials were measured under voltage-clamp conditions at potentials from -90 to -40 mV. Photocurrents were measured at both peak and steady-state points, and reversal potentials were calculated at the membrane potential where the photocurrent amplitude was 0 pA. Current-clamp recordings were carried out at rest.

Resting membrane potential was measured at break-in after reaching whole-cell configuration. When action potentials (AP) were evoked by pulsed current injections, AP inhibition probability was calculated as the % of electrically-evoked spikes that were blocked during the blue 4 s (cultured rat hippocampus neurons) or 10 s (acute slice recordings) light pulse. When APs were evoked by continuous current injections, AP frequency was calculated by measuring spike frequency before (pre, 0.5 s), during (light, 10 s), and after (post, 1 s) light application. Current injection refers to the electrical current amplitude used to evoke action potentials at the different pulse widths. Action potentials were generated by continuous or pulsed current injections. In mPFC neurons, the utilized electrical pulse protocols applied either 10 or 20 Hz pulse trains with either 30 ms pulse widths and current injections at 235 pA ± 15, or 10 ms pulse widths and current injections at 427 pA ± 34, or 5 ms pulse widths and current injections at 720 pA ± 43. In hippocampal PV+ interneurons pulsed current injections were applied at 20 Hz with amplitudes at 360 pA ± 52 (10 ms pulse width) and at 423 pA ± 47 (5 ms pulse width). In dopaminergic neurons in substantia nigra pulsed electrical current injections were applied between 5 and 10 Hz with amplitudes at 342 pA ± 38 (10 ms pulse width). Cells from dorsal root ganglion were excited by 10 ms pulses at 10 Hz (241 pA ± 27). Current injections were individually titrated for each cell and chosen based on minimal amplitudes necessary to reach threshold for action potential generation. Pulsed currents were applied for 12 seconds with a 10 s light inhibition period in between. V_{AP} was measured individually for each cell at the voltage deflection point at which the first-order derivative of the membrane potential (dV/dt) exhibited a sharp transition, typically > 10mV/ms. Input resistance was measured from the steady-state current response after a -20 mV voltage step with and without opsin activation. Cell capacitance was calculated using the integral

of the area under the transient charge after a -20 mV voltage step. Series resistance was continuously monitored throughout the recordings for stability (<20% change) or cells were omitted otherwise. Furthermore, cells were omitted when the leak current was or became larger than 150 pA.

For iC++ and eNpHR3.0 comparisons in pyramidal neurons of mouse mPFC, 10 ms pulsed current injections were applied between the minimum current necessary to evoke action potentials and the maximum current which could be inhibited during a 10 s light application. Pulsed current injections were applied for 12 seconds with one second periods before and after light application. Continuous current injections were applied between 0 pA and either the maximum current which depolarized the cell to depolarization block potential during light application or the maximum current which could be inhibited during a 2 second light application. Continuous currents were injected for 2.5 seconds with 250 ms periods before and after light application. Current amplitudes were increased from 0 – 300 pA in 25 pA steps, from 300 to 900 pA in 50 pA steps and from 1000 to maximum in 100 pA steps. Depolarization block potential was measured by large continuous current injections without light application and determined as the potential at which cell membranes stabilize after they stop firing action potentials.

For the TGOT experiments, the membrane potential was calculated at baseline (pre), during application of TGOT (TGOT), and after TGOT wash-out (post). The membrane potential change induced by blue light during the TGOT application was measured at both the peak and steady state points after light application. Inhibition probability was calculated as the % of cells in which blue light inhibited TGOT-induced cell firing.

An upright microscope (BX61WI, Olympus) with infrared differential interference contrast (IR-DIC) optics was used for neuronal *in vitro* electrophysiological recordings. A Spectra X Light engine (Lumencor) attached to the fluorescent port of the microscope used for viewing eYFP expression and for opsin activation/deactivation. 475/15, 586/20, and 632/22 filters were used for blue, yellow, red light, respectively (Chroma). Light power through the objective was measured with a power meter (ThorLabs). Data was obtained using a MultiClamp700B amplifier, 1440A Digidata digitizer, and pClamp10.3 software (Molecular Devices), and pClamp10.3, OriginLab8 (OriginLab), and SigmaPlot (SPSS) were used for data analysis.

Histology for patch clamp recordings:

Histology was performed at least 4 weeks after injection of viruses. Mice were first transcardially perfused with ice-cold PBS, then immediately perfused with 4% paraformaldehyde (PFA). Brains were fixed overnight in PFA, then placed in a 30% sucrose/PBS solution. 40 μm sections of the brain slices from the various injected regions were prepared using a freezing microtome (Leica), and stored in cryoprotectant (25% glycerol, 30% ethylene glycol, in PBS) until further processing. For 4',6-diamidino-2-phenylindole (DAPI) staining, slices were first washed in PBS, then incubated for 20 minutes with DAPI at 1:50,000. They were then washed again in PBS, and mounted using PVA-DABCO (Sigma). A scanning confocal microscope (DM600B, Leica) and LAS AF software (Leica) was used for obtaining and analyzing images. Histology was performed once per experimental group, but animals were taken from the same groups that were used for in vitro and in vivo electrophysiology. Therefore images represent a randomly picked animal from a group of n = 9 (iC++ in mPFC, Fig. 3a), n = 5 (iC++ in hippocampus, Fig. 4a) and n = 5 (SwiChR++ in mPFC, Supplementary figure 5).

Data analysis for patch clamp recordings:

Electrophysiological data was analyzed using Clampfit 10.4 and Origin 9. All data are given as mean ± standard error of the mean. Initial photocurrents (I_0) were determined by linear extrapolation to $I(t=0)$. Reversal potentials were calculated by linear fit of the two data points between crossing of I=0 pA occurs. For the action spectra recording photocurrents have been normalized to the maximum response. The maximum response wavelength (λ_{max}) has been determined by fitting single recorded action spectra with a three parametric Weibull function.

***In vivo* recording with optogenetic manipulation of PV interneurons in mPFC**

For virus injection, animals (8 weeks of age, 2 PV-Cre mice) were anaesthetized with isoflurane (2%) in O_2 and fixed in a stereotaxic apparatus (MyNeurolab). A small craniotomy was made bilaterally above mPFC (1.76 mm anterior to Bregma, and 0.25 mm lateral to midline) and virus (AAV8-EF1a-DIO-iC++-EYFP, 0.5 µl) was injected into the mPFC (PL/IL). The animals were injected with analgesic (Buprenorphine 0.1 mg/kg s.c.) at the end of surgery.
In vivo extracellular recordings were performed on anesthetized animals 4-5 weeks after virus injection. For the recordings, 32-channel silicon probes (4 shanks with 2 tetrodes, NeuroNexus) and a Digital Lynx 4SX acquisition system with Cheetah data acquisition software (Neuralynx) were used. A craniotomy was made above the injection site and the silicon probe was targeted to mPFC and blue light (473 nm, 5 mW at the fiber tip, 4 or 5 s duration) was delivered via an optical fiber (200 µm) placed at the surface of the target brain area. The optical fiber was connected to a patch cable (Doric Lenses) coupled to a blue DPSS laser (Cobolt MLD^{TM} 473 nm, Cobolt) controlled by custom software written in LabView. Unit signals were amplified with the gain of 10,000, filtered with bandwidth 600-6,000 Hz, digitized at 32 kHz. Single units were manually sorted and identified by various spike waveform features using MClust offline sorter (A.D. Redish). Only well-isolated units (8) with isolation distance > 15, L-ratio < 0.2, and the spikes < 0.01% at ISI < 2 ms were included in the data analysis.
To examine optogenetic modulation of PV interneurons, raster and peri-event time histograms (PETHs) were made for each neuron.

Place aversion by inhibition of ventral tegmental area in mice:

Surgery

12 male DAT:Cre mice (9) >8 weeks old at the start of the experiment, were group-housed in a light-regulated colony room (lights on at 7:00am, off at 7:00pm). Food and water were available *ad libitum* for the duration of the experiment. Standard stereotaxic procedures were used to infuse virus and implant optical fibers under ketamine/dexmedetomidine anesthesia. All coordinates are relative to skull surface and bregma in mm. 1 µl of virus was unilaterally infused into the VTA near the midline (AP -2.8, ML +0.3, DV-4.4) and optical fibers (200 µm diameter, 0.39 NA) were bilaterally implanted dorsal to the VTA (10˚ angle, AP-2.8, ML ±1.2, DV -4.1). Virus was injected at a rate of 100 nl/min and the injection pipette was left in place for 5 minutes following each infusion before it was slowly removed. Optical fibers were encased in Geristore dental epoxy (DenMat) which was secured to the skull via metal screws (Antrin Miniature

Specialists). Viral vectors, titers and sources were as follows: AAV_8-Ef1α-DIO-iC++-eYFP, 4.7 x 10^{12}, Stanford Gene and Viral Vector Core; AAV_5-Ef1α-DIO-eNpHR3.0-eYFP, 4.8 x 10^{12}, UNC Vector Core; AAV_5-Ef1α-DIO-eArch3.0-eYFP, 3.4 x 10^{12}, UNC Vector Core.

Real-time place aversion

Behavioral tests were conducted approximately 4 weeks post-surgery. The real-time place aversion assay was performed in a rectangular arena (68 cm x 24 cm) that was divided into two compartments via an opaque barrier that partially bisected the arena, permitting free movement between chambers. For all tests, mice were gently attached to optical patch cables connected to an upstream laser (Laserglow/Shanghai Dream Laser) via an optical commutator (Doric Lenses). The laser was turned off for the 0 mW test. After the optical patch cables were attached, mice were confined to the non-light-paired compartment for 2 minutes to allow them to habituate to the testing conditions. Subsequently, the barrier was removed and mice were given free access to the entire arena for the remainder of the experiment. Every time the mouse crossed into the light-paired compartment, the laser (473 nm for iC++ group; 532 nm for NpHR/Arch groups) was activated via a TTL trigger box (BIOBSERVE), providing continuous illumination at the specified light power for as long as the subject remained in the light-paired compartment. A video tracking system (BIOSERVE) recorded all movements and quantified the amount of time spent in the light-paired compartment, which was reported as a percentage of the total assay duration (20 min). The place aversion test was repeated (24hr between tests) at each light intensity for each mouse. To minimize behavioral generalization, visual and tactile cues were changed each day so that each light power was experienced in a distinct context.

Histological procedures

Mice were deeply anesthetized with sodium pentobarbital and transcardially perfused with 4% paraformaldehyde. Brains were removed, post-fixed for 24 hours and sectioned at room temperature on a vibratome. Free-floating 60 μm sections were processed for tyrosine hydroxylase (TH) and YFP immunohistochemistry. Sections were incubated in a blocking solution (BS) containing bovine serum albumin and Triton X-100 (each 0.2%) in PBS for 20 min. Normal donkey serum (NDS) (10%) was added to BS for a further 30 min incubation. Sections were then incubated overnight with primary antibodies, followed by a 2 h incubation with secondary antibodies (all at room temperature). Sections were then washed and mounted on microscope slides, and coverslipped with Fluoromount G mounting medium (Southern Biotech). Concentrations and sources for antibodies were as follows: rabbit anti-TH 1:1500 (Millipore, #AB152), mouse anti-GFP 1:1500 (Invitrogen, A11120), donkey anti-rabbit AlexaFluor647 and donkey anti-mouse AlexaFluor594, both 1:200 (Invitrogen). Sections were visualized on a Nikon A1 confocal microscope.

Inhibition of conditioned fear response in mice:

Mice

Male and female adult (2-4 months) F1 hybrid (C57BL/6N Tac X 129S6/SvEv Tac) mice were group housed (4 per cage) on a 12 h light/dark cycle. Behavioral experiments were conducted during light-phase. Food/ water were available ad libitum. All procedures were conducted in accordance with policies of the Hospital for Sick Children Animal Care and Use Committee and

conformed to both the Canadian Council on Animal Care (CCAC) and National Institutes of Health (NIH) Guidelines on the Care and Use of Laboratory Animals.

HSV Vectors

Wild-type full-length CREB (kindly provided by Dr. Satoshi Kida, Tokyo University of Agriculture, Tokyo, Japan), iC1C2-EYFP, iC++-EYFP and eNpHR3.0-EYFP cDNAs were subcloned into a bi-cistronic HSV vector backbone designed for short-term expression (HSV-p1006). In this vector, CREB expression is driven by the HSV immediate-early gene IE 4/5 promoter and the opsin by a CMV promoter. Transgene expression using this viral system typically peaks 3 d following microinjection (10-13). Average titer of the virus stocks was 4.0×10^7 infectious units/ml. When microinjected into the LA, HSV primarily infects principal pyramidal cells (CaMKIIα+ cells) and 3 d post-microinjection we observed no evidence of retrograde transport (14).

Surgery

Mice were pre-treated with atropine sulfate (0.1 mg/kg, ip), anesthetized with chloral hydrate (400 mg/kg, ip) and placed in a stereotaxic frame. Skin was retracted and holes drilled in the skull bilaterally above the LA (AP = -1.4, ML = ±3.5, DV = -5.0 mm) (15). Viral vector (1.5 µl/side) was microinjected through glass micropipettes connected via polyethelene tubing to a microsyringe (Hamilton, Reno, NV) at a rate of 0.1 µl/min. Micropipettes were left in place an additional 5 min following microinjection to ensure diffusion of vector. In-house constructed optical fibres were implanted just dorsal to the LA (11). Mice were treated with analgesic (ketoprofen, 5 mg/kg, sc).

Histology

Four days following vector microinjection, mice were transcardially perfused with 4% paraformaldehyde. Brains were fixed overnight (4°C) and coronal brain slices (50 µm) across the entire anterior-posterior extent of LA were collected using a vibratome. Visualization of transgene expression was enhanced using a primary antibody directed against YFP (rabbit anti-GFP Molecular Probes, A11122, 1:1000) and an Alexa fluor 488-conjugated secondary antibody (goat anti-rabbit IgG, Molecular Probes, A11034, 1:1000). Every second section was mounted on a gelatin-coated glass slide and coverslipped with fluorescence mounting medium containing DAPI (Vector Laboratories Inc., Burlingame, CA). Consistent with previous reports from several labs, microinjection of HSV vectors produces robust localized transgene expression with minimal tissue damage around the site of microinjection. Immunofluorescence (which did not differ across vectors) was used to determine placement and extent of the viral infection for each mouse. Based on this, each mouse was classified as a "hit" or "miss" by an examiner unaware of the treatment condition and behavioral results for that mouse. Mice were defined as "hits" if robust bilateral EYFP expression was observed in LA in at least 5 consecutive brain sections (across the anterior-posterior plane) and if the fiber optic was implanted directly above this. Only mice determined to be a bilateral "hit" were included in subsequent data analysis.

Fear training and testing

Fear conditioning training consisted of placing mice in a conditioning chamber and, 2 min later, presenting a tone (2800 Hz, 85 dB, 30 sec) that co-terminated with a shock (2 sec, 1.0 mA).

Mice remained in chamber for an additional 30 sec. Behavior was monitored by overhead cameras, which digitized video images at 4 Hz. Reactivity to shock was assessed by comparing distance travelled in 2 s prior to shock onset (pre-US), to distance travelled during the 2 s-shock (US). Reactivity Index = (US - pre-US) / (US + pre-US). Importantly, we observed no difference in shock reactivity between vectors.
The memory test occurred 24 h later. The percentage of time mice spent freezing to the tone CS was assessed both with and without light stimulation (counterbalanced). Two min following placement in a novel chamber, the CS (1 min) was presented twice, with a 2-min intervening interval. During one CS presentation, blue light (10 mW square pulse throughout 1 min tone) was also delivered. Because the tethered optical fiber reduced the accuracy of the automated analysis, freezing was scored by two experimenters unaware of the treatment condition. Scores were averaged.

Statistical analysis:

We did not predetermine sample sizes, but used sample sizes that were used in prior studies, reflect the standards in the field and which ensure statistical significance for all applications. $P<0.05$ is defined to be statistically significant. No randomization or blinding was conducted during the experiments. Origin 9.1 and Matlab software were used for statistical analysis. Data sets were tested for normality and equal variances. We used an unpaired, two tailed t-test and for the comparison of two data sets and one-way or two way ANOVA followed by a Dunn-Sidak or Tukey's post-hoc analysis for multiple data-sets. A Welch correction was included in case of unequal variances. We used a Mann-Whitney test for nonparametric statistics. For the inhibition of fear memory in mice, the amount of time spent freezing to the tone in the presence or absence of blue light (within subject variable) was compared across virus groups (between subject variable) by ANOVA. For tone fear memory, we analyzed the time spent freezing during the tone. Amount of time spent freezing was compared across groups by Analysis of Variance (ANOVA) and significant effects were further analyzed using Newman-Keuls post-hoc tests. Tables for all statistical tests are provided below.

```
C1C2          1     MSRRPWLLALALAVALAAGSAGASTGSDATVPVATQDGPDYVFHRAHERMLFQTSYTLENNGSVICIPNNGQCFCLAWLKSNGTNAEKLAANILQWITFALSALCLMFYGYQTW
iC1C2         1     MSRRPWLLALALAVALAAGSAGASTGSDATVPVATQDGPDYVFHRAHERMLFQTSYTLENNGSVICIPNNGQCFCLAWLKSNGTNAEKLAANILQWISFALSALCLMFYGYQTW
iC++          1     ----------------------------------------MDYGGALSAVGLFQTSYTLENNGSVICIPNNGQCFCLAWLKSNGTNAEKLAANILQWISFALSALCLMFYGYQTW
SwiChR++      1     ----------------------------------------MDYGGALSAVGLFQTSYTLENNGSVICIPNNGQCFCLAWLKSNGTNAEKLAANILQWISFALSALCLMFYGYQTW
GtACR2        1     -------------------------------------------------MASQVVYG-EWASTHTECYNMS--------------RIDSTFVSLLQLVWAVVSGCQTIFMISRA

C1C2          115   KSTCGWEEIYVATIEMIKFIIEYFHEFDEPAVIYSSNGNKTVWLRYAEWLLTCPVILIHLSNLTGLANDYNKRTMGLLVSDIGTIVWGTTAALS-KGYVRVIFFLMG---LCYG
iC1C2         115   KSTCGWEEIYVATISMIKFIIEYFHSFDEPAVIYSSNGNKTKWLRYASWLLTCPVILIRLSNLTGLANDYNKRTMGLLVSDIGTIVWGTTAALS-KGYVRVIFFLMG---LCYG
iC++          76    KSTCGWENIYVATIQMIKFIIEYFHSFDEPAVIYSSNGNKTRWLRYASWLLTCPVILIHLSNLTGLANDYNKRTMGLLVSDIGTIVWGTTAALS-KGYVRVIFFLMG---LCYG
SwiChR++      76    KSTCGWENIYVATIQMIKFIIEYFHSFDEPAVIYSSNGNKTRWLRYASWLLTAPVILIHLSNLTGLANDYNKRTMGLLVSDIGTIVWGTTAALS-KGYVRVIFFLMG---LCYG
GtACR2        51    PKVP-WESVYLPFVESI----TYALASTGNGTLQMRDGRFFPWSRMASWLCTCPIMLGQISNMALVKYKSIPLNPIAQAASIIRVVMGITATISPAEYMKWLFFFGATCLVFE

C1C2          225   IYTFFNAAKVYIEAYHTVPKGRCRQVVTGMAWL---FFVSWGMFPILFILGPEGFGVLSVYGSTVGHTIIDLMSKNCWGLLGHYLRVLIHEHILIHGDIRKTTKLNIGGTEIEV
iC1C2         225   IYTFFNAAKVYIEAYHTVPKGRCRQVVTGMAWL---FFVSWGMFPILFILGPEGFGVLSKYGSNVGHTIIDLMSKQCWGLLGHYLRVLIHEHILIHGDIRKTTKLNIGGTEIEV
iC++          186   IYTFFNAAKVYIEAYHTVPKGRCRQVVTGMAWL---FFVSWGMFPILFILGPEGFGVLSRYGSNVGHTIIDLMSKQCWGLLGHYLRVLIHSHILIHGDIRKTTKLNIGGTEIEV
SwiChR++      186   IYTFFNAAKVYIEAYHTVPKGRCRQVVTGMAWL---FFVSWGMFPILFILGPEGFGVLSRYGSNVGHTIIDLMSKQCWGLLGHYLRVLIHSHILIHGDIRKTTKLNIGGTEIEV
GtACR2        160   YSVVFTIFQVGLYGFESVGTPLAQKVVVRIKMLRLIFFIAWTMFPIVWLISPTGVCVIHENVSAILYLLADGLCKNTYGVILWSTAWGVLEGKWDPACLPGQEKPEADDPFGLN

C1C2          336   ETLVEDEAEAGAV----------------------------------------------
iC1C2         336   ETLVEDEAEAGAV----------------------------------------------
iC++          297   ETLVEDEAEAGAV----------------------------------------------
SwiChR++      297   ETLVEDEAEAGAV----------------------------------------------
GtACR2        274   HEKNAPPNDEVNIRMFGRVIGSVRKSKRRQKWELAPAHLEDRIRLSDEESDDSRPKR
```

Supplementary figure 1 Protein sequences of C1C2, iC1C2, iC++ and SwiChR++, Channelrhodopsin-2 (ChR2) and GtACR2. First 50 amino-acids of C1C2 were replaced by first 11 amino-acids of channelrhodopsin-2 (marked in green) for improved membrane trafficking and expression in iC++ and SwiChR++. Mutations in iC1C2, iC1C2++, SwiChR++ are marked in red. Four key residues which face the ion conducting pore and presumably contribute to anion selectivity in GtACR2 are marked in blue.

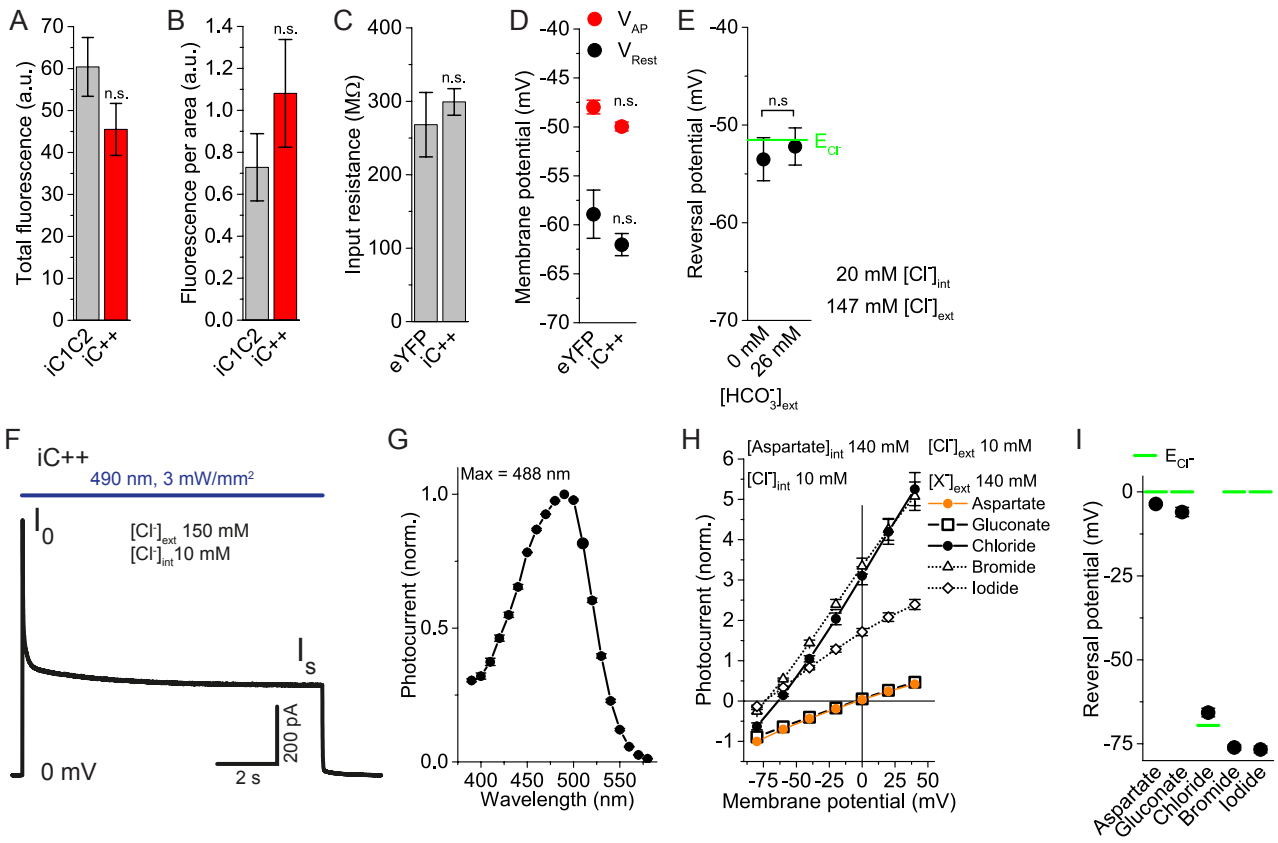

Supplementary figure 2 iC++ characterization in cultured neurons and HEK293 cells **(A)** Total fluorescence of eYFP tagged iC++ and iC1C2 expressed in cultured neurons of rat hippocampus. **(B)** Fluorescence per area depicts the expression density of iC1C2 and iC++ in cultured neurons. **(C)** Input resistance, **(D)** resting membrane potential (V_{Rest}) and threshold for action potential generation (V_{AP}) in eYFP and iC++ expressing cultured neurons. **(E)** Reversal potential of iC++ with and without 26 mM extracellular bicarbonate ($[HCO^-_3]_{ext}$) at equal chloride gradients. No change in the reversal potential was recorded and therefore, bicarbonate conduction was excluded. **(F)** In HEK293 cells, iC++ photocurrent during 10 s light application (blue bar) at 0 mV membrane potential. I_0: peak current, I_S: stationary current. **(G)** Action spectrum of iC++ with maximum wavelength at 488 nm. **(H)** iC++ current amplitudes under external solutions with varying anion composition (X^- 140 mM + 10 mM Cl^-) measured in HEK293 cells. Internal solution: 140 mM Aspartate and 10 mM Cl^-. **(I)** Reversal potentials from (G) in relations to the Nernst chloride equilibrium (green bar). (n.s.: P > 0.5, Error bars: s.e.m, all values and N's are listed in Supplementary Table 8).

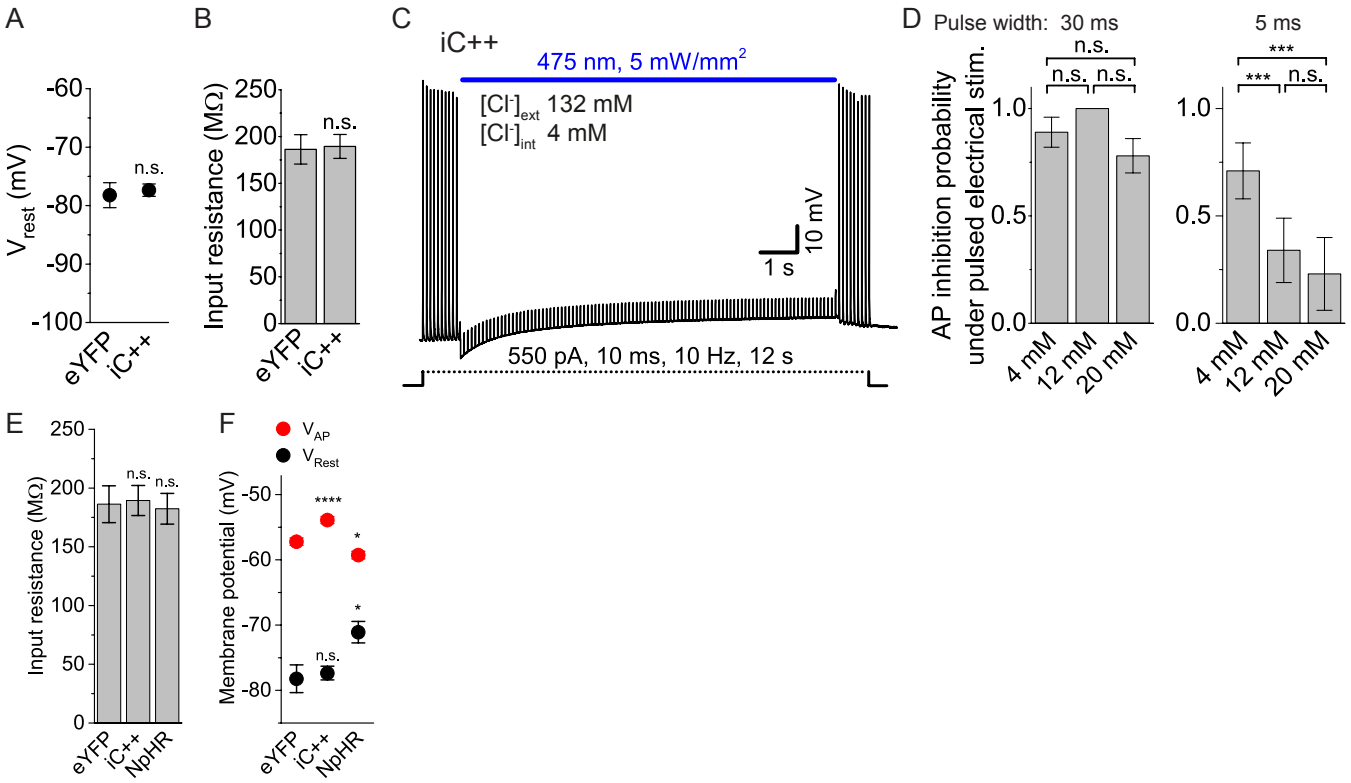

Supplementary figure 3 Chloride-dependent inhibition of pyramidal neurons in mouse mPFC. **(A)** Resting membrane potential and **(B)** input resistance in cells expressing eYFP and iC++. **(C)** Voltage trace of iC++ expressing neuron showing AP generation by pulsed current injections (dotted line) and inhibition during 10 s light application (blue bar). **(D)** Inhibition probability of APs evoked by pulsed current injections and at varying pulse widths. Electrical inputs were individually titrated to the action potential (AP) threshold (average: 30 ms: 250 ± 18 pA; 5 ms: 740 ± 84 pA) and applied at 10 Hz for 12 s, light was on for 10 s. **(E)** Input resistance, **(F)** resting membrane potential and threshold for AP generation in cells expressing eYFP and iC++ compared to NpHR. (n.s.: P > 0.5, *P < 0.05, ***P < 0.005, ****P < 0.0001, Error bars: s.e.m, all values and N's are listed in Supplementary Table 8).

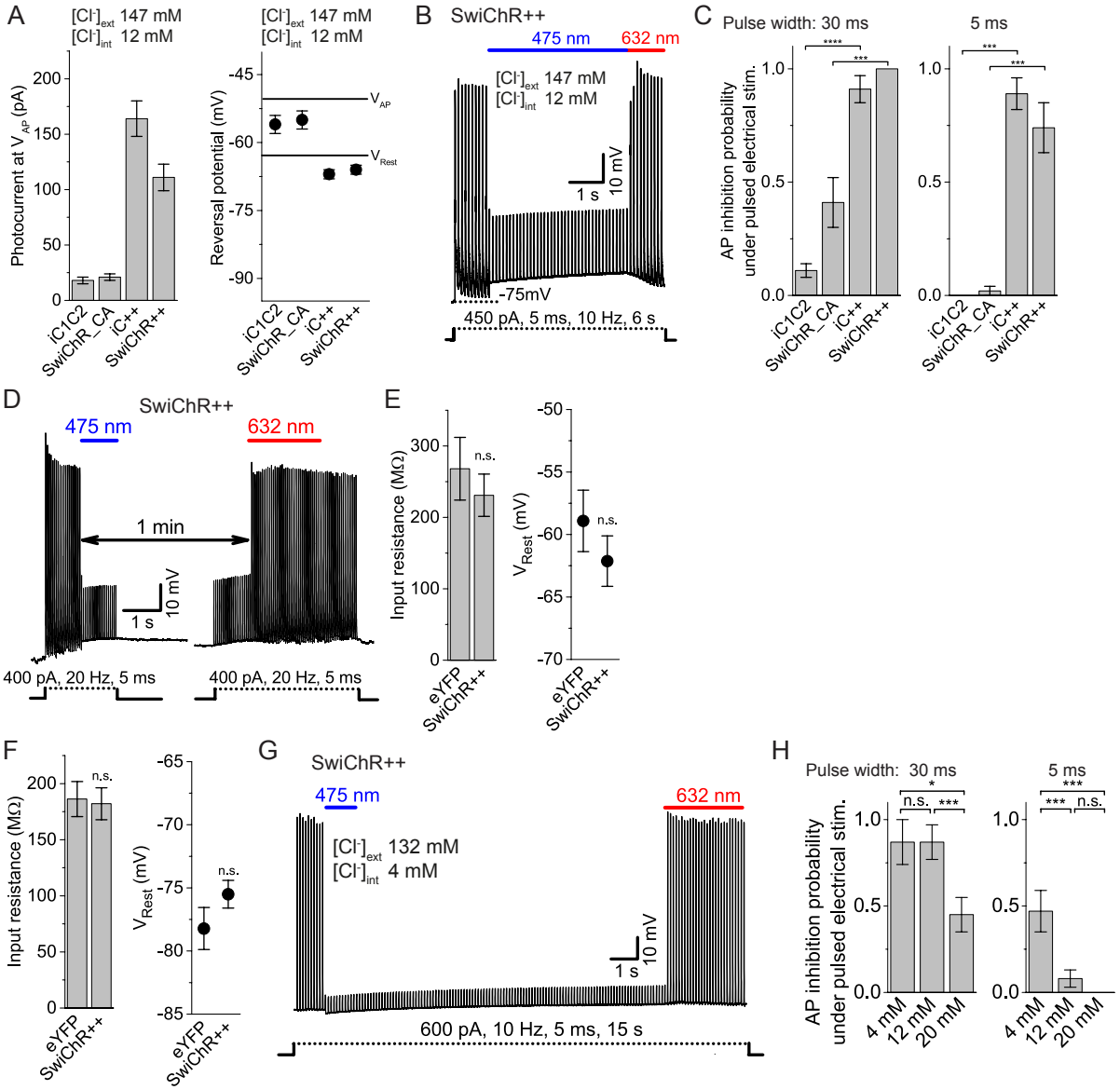

Supplementary figure 4 SwiChR++ characterization cultured neurons and pyramidal neurons from mPFC. **(A)** Left: Photocurrent amplitudes measured at threshold for action potentials (V_{AP} = -50 mV ± 1) and, right: reversal potentials of chloride selective channelrhodopsins. Measured at 12 mM intracellular chloride concentration in cultured neurons. **(B)** Voltage trace of cultured neuron expressing SwiChR++. Action potentials (AP) were evoked by pulsed current injections at 10 Hz (dotted line) and inhibited by a continuous blue light pulse (blue bar) for 4 s. SwiChR++ was deactivated by a continuous red light pulse which recovered spiking. **(C)** Inhibition probability of APs evoked by pulsed current injections (6 s, 10 Hz) with 30 ms (left), and 5 ms (right) pulse width under 4 s light application. Current injections were individually titrated to V_{AP}: 30 ms, average: 186 ± 16 pA and 5 ms: 503 ± 42 pA. **(D)** Voltage trace of cultured neuron expressing SwiChR++. Pulsed current injections were applied for 2 s at 20 Hz. SwiChR++ was activated 1 second upon AP generation by a blue light pulse (blue bar) which inhibited spiking. SwiChR++ remained active for one minute as seen by inhibited spiking during a second train of current injections. AP generation recovers upon SwiChR++ deactivation caused by red light pulse (red bar). **(E)** Left: Input resistance and, right: resting membrane potential of SwiChR++ and eYFP expressing cultured neurons. **(F)** Left: Input resistance and, right: resting membrane potential of SwiChR++ and eYFP expressing pyramidal neurons from mouse mPFC. **(G)** Voltage trace of SwiChR++ expressing pyramidal neuron showing AP generation by pulsed current injections (dotted line, 10 Hz, 15 s) and 12 s inhibition upon 1 s blue light application (blue bar). Spiking recovers upon red light application (red bar). **(H)** Inhibition probability of APs evoked by pulsed current injections with 30 ms and 5 pulse widths. Current injections were individually titrated to V_{AP} average 30 ms: 223 ± 31 pA and 5 ms: 560 ± 74 pA. (n.s.: P > 0.5, *P < 0.05, ***P < 0.005, ****P < 0.0001, Error bars: s.e.m, all values and N's are listed in Supplementary Table 8).

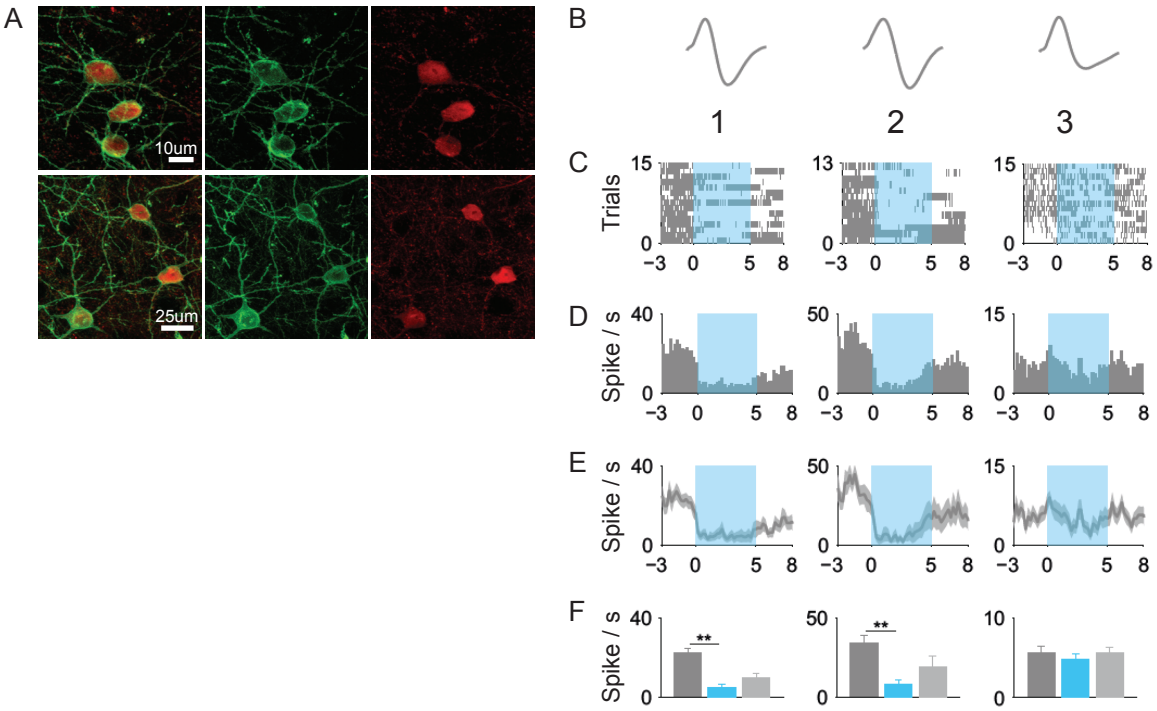

Supplementary figure 5 Inhibition of spontaneous activity in iC++ expressing PV+ interneurons in mPFC of anesthetized mouse. **(A)** Confocal images of PV-Cre mice expressing iC++ in PV+ neurons in mouse mPFC. 97.7% stained for PV (EYFP+ (green)/PV+ (red) 905 cells, EYFP+/PV- 21 cells), 93.4% of PV cells expressed EYFP (EYFP+/PV+ 905 cells, EYFP-/PV+ 64 cells), n = 2, 10 – 11 sections counted for each animal. **(B)** Inhibition of spontaneous single unit activity in mPFC-PV+ cells by 5 s light application. Average waveform of sorted spikes. Cell 1 and cell 2 waveforms are typical for PV+ interneuron and cell 3 waveform is typical for cortical pyramidal neurons. **(C)** Raster plots, **(D)** peri-event time histograms of spikes and **(E)** average spike frequency of neurons in response to a blue light exposure (blue area). Note, cell 3 does not significantly reduce spike frequency in response to light. **(F)** Average spike frequencies pre, during and post light stimulation. (**P < 0.01, Error bars: s.e.m, all values and N's are listed in Supplementary Table 8).

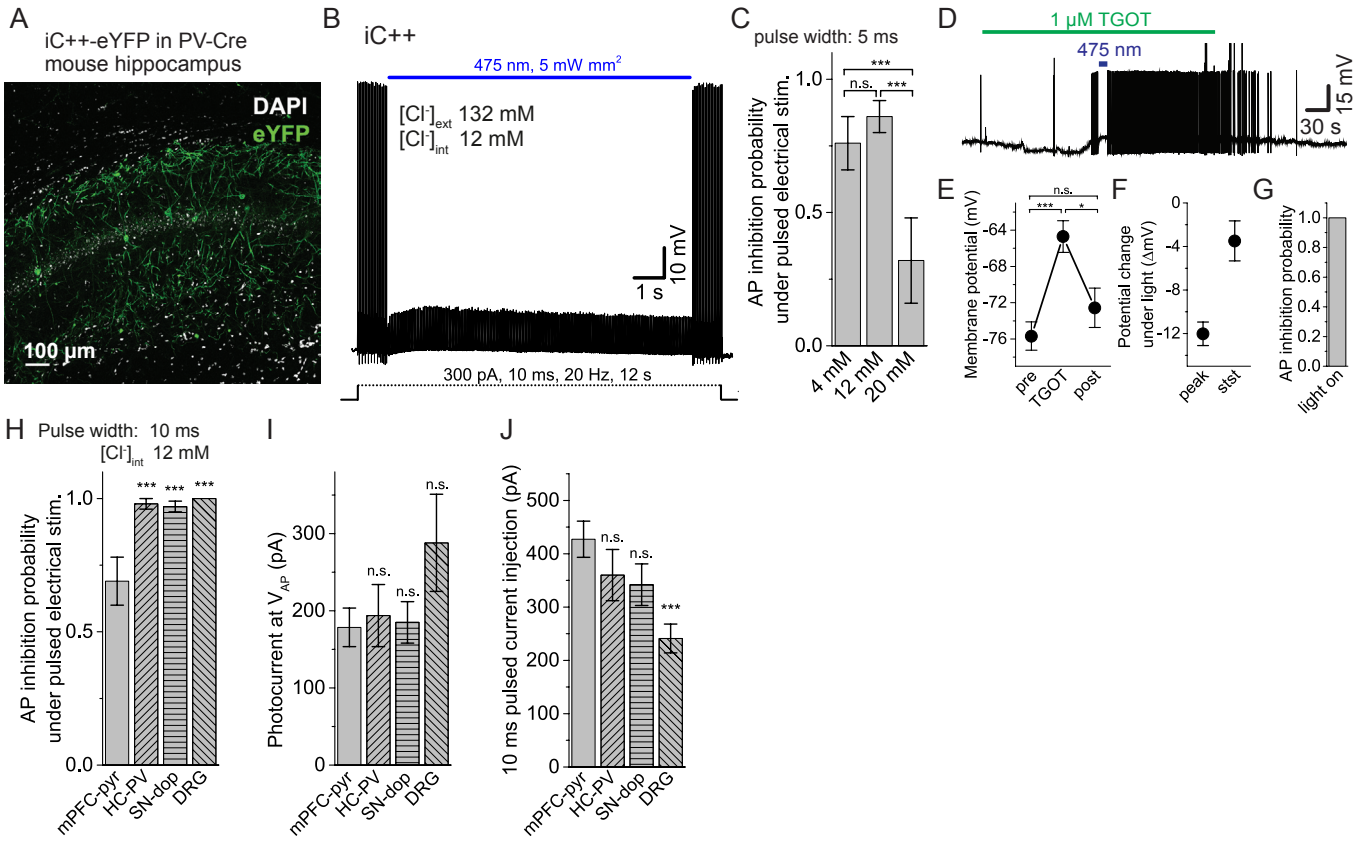

Supplementary figure 6 iC++-mediated inhibition in various cell types and brain regions. **(A)** Confocal image of iC++ expression in PV+ interneurons of hippocampus from PV-Cre mouse, 5 weeks post virus-injection. **(B)** Voltage trace of iC++-expressing fast-spiking interneuron. Action potentials (AP) were evoked by electrical current injections at 20 Hz (dotted line). Spiking was inhibited during 10 s light application (blue bar). **(C)** Inhibition probability of electrically-evoked APs (20 Hz, 12 s) at 5 ms pulse width. Light was on for 10 s. Current inputs were titrated individually to reach AP threshold, average: 423 ± 47 pA. **(D)** Voltage trace of iC++-expressing hippocampal PV+ neuron showing increased spiking upon external Thr4-Gly7-oxytocin application (TGOT, green bar). Spiking is inhibited during 10 s light application (blue bar). **(E)** Membrane potential of iC++-expressing PV+ neurons pre, during and post TGOT application (no light). **(F)** Light-induced membrane potential change during TGOT application in PV+ neurons and **(G)** total inhibition probability during light application. **(H)** Inhibition probability in mPFC pyramidal neurons, hippocampal PV+ neurons, dopaminergic neurons in substantia nigra and cultured peripheral DRG neurons. Cells were excited by pulsed electrical current injections (10 ms) at frequencies between 5 and 20 Hz and inhibited by 10 s light application ($[Cl^-]_{int}$ = 12 mM). Current injections were individually titrated to reach AP threshold. **(I)** iC++ photocurrents at AP threshold (VAP, measured 1 s upon light application). **(J)** Average current amplitudes used for AP generation in (H). (n.s.: P > 0.05, *P < 0.05, ***P < 0.005, Error bars: s.e.m, all values and N's are listed in Supplementary Table 8).

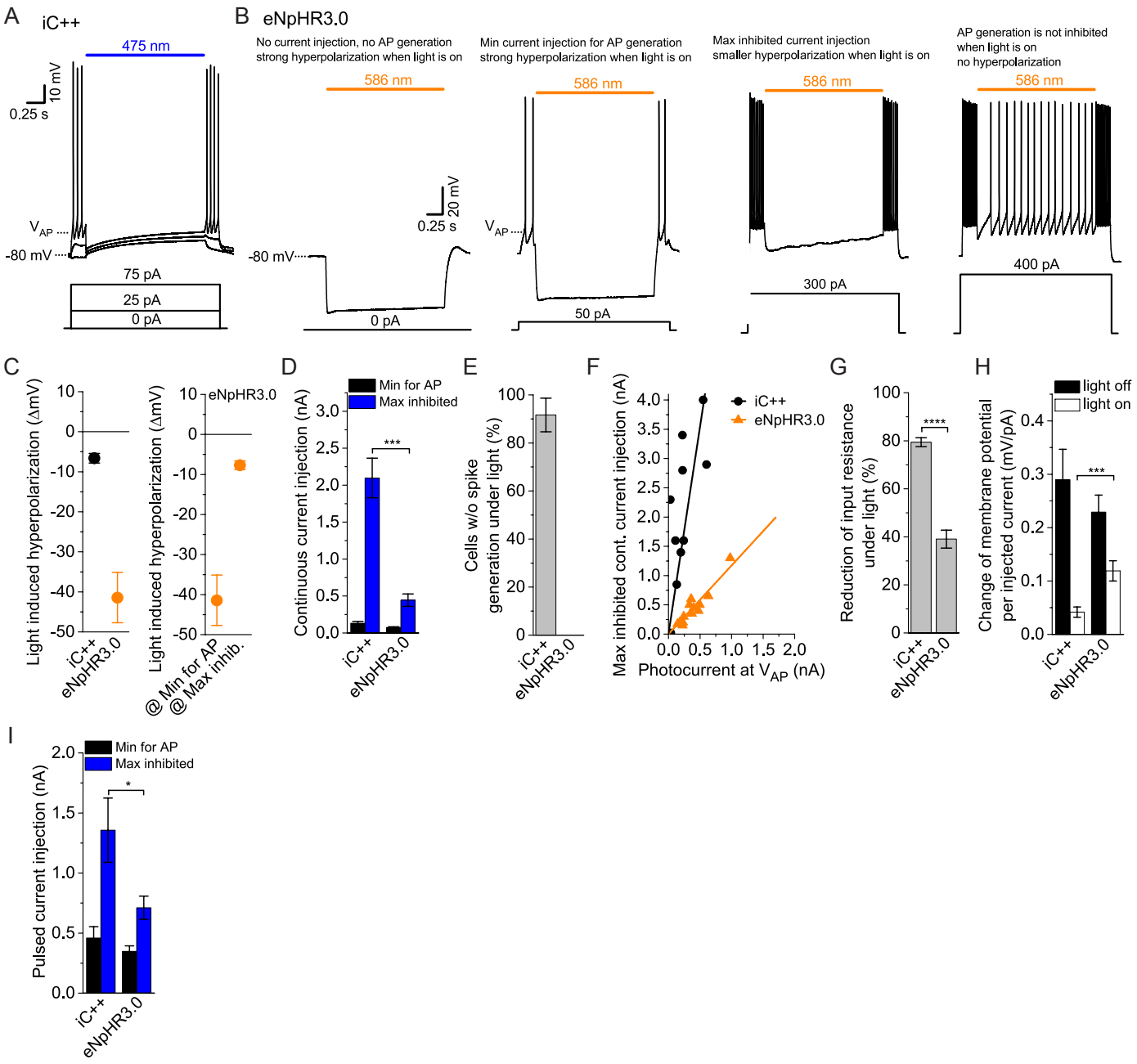

Supplementary Figure 7 iC++ inhibition efficiency in mPFC pyramidal cells compared to eNpHR3.0. **(A)** Voltage traces of representative iC++ expressing cell in response to continuous electrical current injection and light delivery (blue bar). Current injection inputs were increased in 25 pA steps. In this case the cell started to spike at 75 pA when membrane depolarization reached threshold for AP generation (V_{AP}). The spikes (APs) were inhibited by iC++ activation with blue light. **(B)** Left, voltage trace of eNpHR3.0-expressing cell hyperpolarized strongly with light delivery (orange bar); no electrical current was injected. Left middle, continuous electrical currents were applied in 25 pA steps to determine the minimum currents for AP generation and the maximum current that could show induced-spike inhibition under light. At the minimum of 50 pA, membrane potential reached AP threshold. Spiking was inhibited by a strong membrane hyperpolarization-inducing eNpHR3.0 activation. Right middle, the level of eNpHR3.0-induced hyperpolarization decreased under increasing current injections (here, 300 pA), but AP generation was still inhibited. Right, at 400 pA stimulation current and above, AP generation could not be blocked by eNpHR3.0. **(C)** Left, light-induced hyperpolarization measured from V_{AP} when the minimum electrical current sufficient for AP generation had been applied. Right, for eNpHR3.0 only: change of membrane potential measured from V_{AP} when the minimum current for AP generation (@ Min for AP), or the maximum current injection at which APs could still be inhibited, had been applied (@ Max inhibited). **(D)** Average minimum current injections to reach V_{AP} (black) compared to maximum current injections at which APs could still be inhibited (blue). Beyond this maximum, cells either started to spike (all eNpHR3.0 cells) or reached depolarization-block potential under light (most iC++ cells). **(E)** Percentage of cells that did not spike under light at any current injection level. Delivered current-injections were not further increased beyond the point at which cells reached depolarization-block potential under light. **(F)** Photocurrents at V_{AP} of individual iC++ (black circles) and eNpHR3.0 (orange triangles) cells plotted against the maximum electrical current injection for which APs could still be inhibited. The slope of the linear fit for eNpHR3.0 (~1, orange line) was considerably lower compared to that for iC++ (~7, solid black line). **(G)** Reduction of input resistance during light delivery. **(H)** Change of membrane potential in response to electrical current injections with (white) and without (black) opsin activation. **(I)** Inhibition efficiency was also tested for APs evoked by pulsed current injections. Current inputs were individually titrated from minimum to reach threshold (black) and compared to the maximum (blue) for which spikes could still be inhibited with 100% efficacy during 10 s light application. Pulsed current injections: 10 ms, 10 Hz, 12 s. All measurements were conducted at 4 mM intracellular chloride concentration (*P < 0.05, ***P < 0.005, ****P < 0.0001, Error bars: s.e.m, all values and N's are listed in Supplementary Table 8).

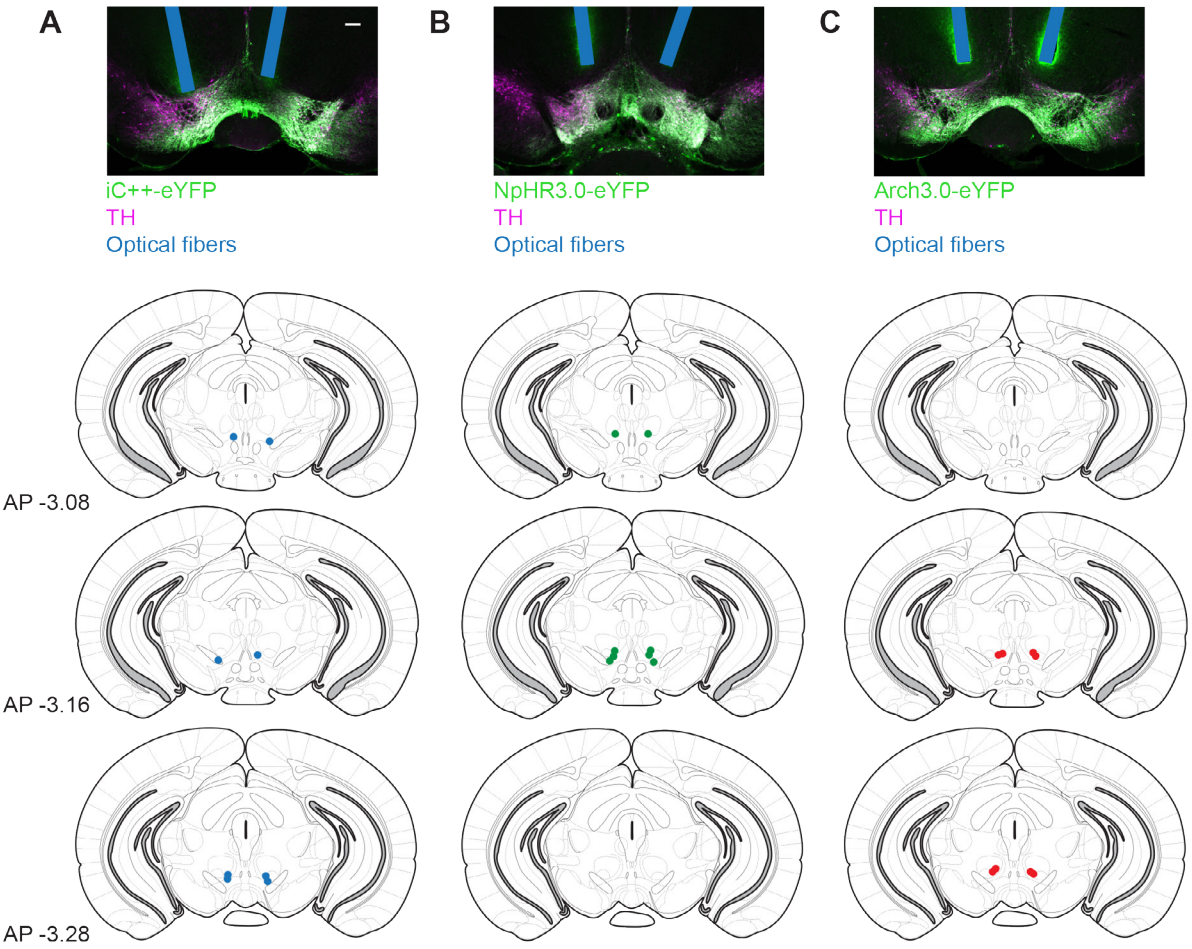

Supplementary figure 8 (A) Top, confocal image showing representative virus expression and optical fiber placement for iC++ group. Bottom, location of optical fiber tips for all mice (n = 4) in iC++ group. **(B)** Top, confocal image showing representative virus expression and optical fiber placement for eNpHR3.0 group. Bottom, location of optical fiber tips for all mice (n = 4) in eNpHR3.0 group. **(C)** Top, confocal image showing representative virus expression and optical fiber placement for Arch group. Bottom, location of optical fiber tips for all mice (n = 4) in Arch group. For A-C (top), scale = 200 μm.

Supplementary Tables

Supplementary Table 1

Supplementary Table for Figure 1A, B, C

$[Cl^-]_{ext}$ 147 mM / $[Cl^-]_{int}$ 4 mM	V_{rev} (mV)	s.e.m.	PC at V_{AP} (pA)	s.e.m.	N*	R_{in} (MΩ)	s.e.m.	N*
iC1C2	-63.5	± 1.1	55	± 6	16,16,3	196	± 12	16,16,3
SwiChR_CA	-68.1	± 1.0	70	± 11	7,7,3	186	± 38	7,7,3
slow ChloC	-67.0	± 1.2	118	± 21	8,8,3	383	± 56	8,8,3
K117R/K242R	-68.4	± 1.2	71	± 11	16,16,3	249	± 35	19,19,3
E83N	-79.8	± 0.3	65	± 7	8,8,3	122	± 15	16,16,3
E83Q	-80.5	± 0.8	41	± 4	6,6,2	150	± 19	6,6,2
E83N/R134H	-76.9	± 0.8	343	± 42	11,11,2	262	± 43	18,18,3
E83Q/R134H	-73.9	± 1.4	174	± 29	9,9,3	318	± 44	13,13,3
E83C/R134H	-77.1	± 1.1	228	± 58	12,12,4	267	± 41	28,28,5
E83S/R134H	-78.2	± 0.8	192	± 22	11,11,3	310	± 70	18,18,5
E83Q/K117R/R134H/K242R	-73.6	± 1.5	188	± 46	7,7,2	259	± 56	7,7,2
E83Q/S90Q/K117R/R134H/K242R	-75.4	± 1.5	206	± 49	11,11,2	321	± 58	22,22,4
E83C/S90Q/K117R/R134H/K242R	-79.1	± 1.0	196	± 39	10,10,2	335	± 69	19,19,3
E83C/S90Q/K117R/R134H/K242R/E273S	-78.3	± 0.8	260	± 43	10,10,2	255	± 51	19,19,4
E83N/S90Q/K117R/R134H/K242R/E273S (iC++)	-78.3	± 0.7	348	± 35	18,18,3	285	± 34	18,18,3

V_{rev}: iC1C2 vs. iC++: P<0.0001, t = 9.63
PC at V_{AP}: iC1C2 vs. iC++: P<0.0001, t = 6.19
R_{in}: iC1C2 vs. E83N: P<0.005, t = 3.71, E83N vs. E83N/R134H: P<0.0001, t = 4.56,
*N: total number of measurements, cells, number of separately prepared and transfected cell culture batches

Supplementary Table for Figure 1D

	PC per fluorescence (a.u.)	s.e.m.	N*
iC1C2	0.48	± 0.11	6,6,1
iC++	7.93	± 1.15	13,13,3

PC per fluorescence: P<0.0001, t = 6.47
*N: total number of measurements, cells, number of separately prepared and transfected cell culture batches

Supplementary Table for Figure 1H

$[Cl^-]_{ext}$ 147 mM / $[Cl^-]_{int}$ 4 mM	Pulse width 30 ms	s.e.m.	Median	Q1	N*
iC1C2 AP inh. prob.	0.34	± 0.09	0.16	0	16,16,3
iC++ AP inh. prob.	1	± 0	1	1	8,8,1

iC1C2 vs. iC1C2 AP inhibition probability: P<0.0001, U = 0
*N: total number of measurements, cells, number of separately prepared and transfected cell culture batches

Supplementary Table for Figure 1H

$[Cl^-]_{ext}$ 147 mM / $[Cl^-]_{int}$ 4 mM	Pulse width 5 ms	s.e.m.	Median	Q1	N*
iC1C2 AP inh. prob.	0.01	± 0.01	0	0	8,8,1
iC++ AP inh. prob.	1	± 0	1	1	15,15,3

iC1C2 vs. iC1C2 AP inhibition probability: P<0.0001, U = 0
*N: total number of measurements, cells, number of separately prepared and transfected cell culture batches

Supplementary Table 2

Supplementary Table for Figure 3C

$[Cl^-]_{ext}$ 150 mM	I_0 V_{rev} (mV)	s.e.m.	I_s V_{rev} (mV)	s.e.m.	N*	E_{Cl} (mV)
$[Cl^-]_{int}$ 10 mM	-66.2	± 0.7	-65.1	± 0.5	11,11,4	-69.5
$[Cl^-]_{int}$ 50 mM	-27.9	± 0.2	-26.5	± 0.2	8,8,2	-28.2
$[Cl^-]_{int}$ 120 mM	-4.0	± 0.2	-3.8	± 1.6	9,9,3	-5.7

*N: total number of measurements, cells, number of separately prepared and transfected cell culture batches

Supplementary Table for Figure 3D

$[Cl^-]_{ext}$ 150 mM $[Cl^-]_{int}$ 10 mM	Change in input resistance under increasing chloride gradient w/o light (norm. to $[Cl^-]_{ext}$ 10 mM)	s.e.m.	N*
iC1C2	0.47	± 0.04	9,9,1
iC++	1.06	± 0.07	9,9,1

iC++ vs. iC1C2: P<0.0001, t = 6.93
*N: total number of measurements, cells, number of separately prepared and transfected cell culture batches

Supplementary Table for Figure 3F

	Photocurrent at pH 5, 0 mV (norm. to pH 7.2)	s.e.m.	N*
iC1C2	1.9	± 0.2	6,6,1
iC++	10.4	± 1.0	6,6,1

iC++ vs. iC1C2: P<0.005, t = 8.63
*N: total number of measurements, cells, number of separately prepared and transfected cell culture batches

Supplementary Table for Figure 3G

$[Cl^-]_{ext}$ 150 mM $[Cl^-]_{int}$ 10 mM	V_{rev} (mV)	s.e.m.	N*
iC++, pH 7.2	-65.5	± 0.6	6,6,1
iC++, pH 5	-65.1	± 1.0	6,6,1
iC1C2, pH 7.2	-61.9	± 1.8	10,10,2
iC1C2, pH 5	-58.1	± 0.5	6,6,1

*N: total number of measurements, cells, number of separately prepared and transfected cell culture batches

Supplementary Table 3

Supplementary Table for Figure 4C, D

$[Cl^-]_{ext}$ 132 mM	V_{rev} (mV)	s.e.m.	PC at V_{AP} (pA)	s.e.m.	N*
$[Cl^-]_{int}$ 4 mM	-65	± 2	206	± 24	13,13,4
$[Cl^-]_{int}$ 12 mM	-56	± 2	95	± 41	8,8,3
$[Cl^-]_{int}$ 20 mM	-50	± 2	17	± 26	8,8,3

*N: total number of measurements, cells and animals used for slice electrophysiology

Supplementary Table for Figure 4E

$[Cl^-]_{ext}$ 132 mM	pre light AP frequency (Hz)	s.e.m.	light AP frequency (Hz)	s.e.m.	post light AP frequency (Hz)	s.e.m.	N*
$[Cl^-]_{int}$ 4 mM	20	± 2	0	± 0	20	± 2	13,13,3
$[Cl^-]_{int}$ 20 mM	18	± 3	0	± 0	17	± 2	8,8,3

4 mM: pre vs. light inhibition probability: P<0.0001, t = -11.68, pre vs. post: P>0.05, t = 0.44, post vs. light: P<0.0001, t = 11.24
20 mM: pre vs. light inhibition probability: P<0.0001, t = -6.12, pre vs. post: P>0.05, t = -0.09, post vs. light: P<0.0001, t = -6.12
*N: total number of measurements, cells and animals used for slice electrophysiology

Supplementary Table 4

Supplementary Table for Figure 5C, D

iC++ τ_{fast} (ms)	s.e.m.	iC++ τ_{slow} (ms)	s.e.m.	Ampl. ratio τ_{fast}	s.e.m.	Ampl. ratio τ_{slow}	s.e.m.	N*	SwiChR++ τ_{off} / dark (s)	s.e.m.	SwiChR++ τ_{off} / 600 nm (s)	s.e.m.	N*
12.1	± 0.4	329	± 18	0.931	± 0.004	0.069	± 0.004	9,9,3	115.5	± 9.0	0.15	± 0.02	7,7,3

N: total number of measurements, cells, number of separately prepared and transfected cell culture batches

Supplementary Table for Supplementary Figure 5G

$[Cl^-]_{ext}$ 132 mM	pre light AP frequ. (Hz)	s.e.m.	light AP frequ. (Hz)	s.e.m.	post light AP frequ. (Hz)	s.e.m.	N*
$[Cl^-]_{int}$ 4 mM	20	± 2	0	± 0	18	± 2	12,12,3
$[Cl^-]_{int}$ 20 mM	14	± 1	0.27	± 0.15	13	± 1	10,10,4

4 mM: pre vs. light inhibition probability: P<0.0001, t = -7.58, pre vs. post: P>0.05, t = 0.83, post vs. light: P<0.0001, t = 6.76
20 mM: pre vs. light inhibition probability: P<0.0001, t = -10.08, pre vs. post: P>0.05, t = -1.03, post vs. light: P<0.0001, t = -9.05
*N: total number of measurements, cells and animals used for slice electrophysiology

Supplementary Table 5

Supplementary Table for Figure 6C

	Time spent in light paired side (0 mW) (%)	s.e.m.	Time spent in light paired side (0.5 mW) (%)	s.e.m.	Time spent in light paired side (5 mW) (%)	s.e.m.	N*
iC++	48.4	5.6	17.0	1.4	9.1	1.5	4
eNpHR3.0	50.0	4.9	15.8	4.1	9.2	1.2	4
Arch3.0	46.0	5.8	13.3	5.2	8.7	1.7	4

main effect of light power: $F_{2, 18}$ = 64.529, P<0.001
Holm-Sidak post-hoc tests: 0 mW vs. 0.5 or 5 mW, P<0.005
no main effect of group: $F_{2, 18}$ = 0.813, P=0.474
no group x light power interaction: $F_{4, 18}$ = 0.0642, P=0.992
*N: total number of measurements and number of animals used

Supplementary Table 6

Supplementary Table for Figure 7c

	Freezing to tone light on (%)	s.e.m.	Freezing to tone light off (%)	s.e.m.	N*
CREB / iC++	14.2	2.1	47.8	4.4	11
iC++	44.3	10.2	49.7	7.3	5
CREB / iC1C2	24.9	4.3	57.0	4.7	12
iC1C2	59.4	7.5	59.0	4.0	6
CREB/NpHR	24.1	3.0	61.2	3.6	9
NpHR	39.8	5.7	42.1	6.8	8
CREB	57.5	6.5	46.8	7.1	8

Light (on, off) x Virus : $F_{6,52}$ = 11.83, p<0.001
Newman-Keuls post-hoc test: CREB/iC++ light on vs. light off, P<0.005; CREB/iC1C2 light on vs. light off, P<0.005;
CREB/NpHR light on vs. light off, P<0.005; iC++ light on vs. light off, P>0.05; iC1C2 light on vs light off, P>0.05; NpHR light on vs light off, P>0.05, CREB on vs light off, P>0.05
CREB/iC++ light on vs. CREB/iC1C2 light on, P>0.05, CREB/iC++ light on vs. CREB/NpHR light on, P>0.05
*N: total number of measurements and number of animals used

Supplementary Table 8

Supplementary Table for Supplementary Figure 2A, B

	Total fluorescence (a.u.)	s.e.m.	Fluorescence per area (a.u.)	s.e.m.	N*
iC1C2	60.4	± 7.0	0.73	± 0.16	6,6,1
iC++	45.5	± 6.2	1.08	± 0.26	13,13,3

Total fluorescence: P>0.05, t = 1.43,
Fluorescence per area: P>0.05, t = 0.89
*N: total number of measurements, cells, number of separately prepared and transfected cell culture batches

Supplementary Table for Supplementary Figure 2C

	R_{in} (MΩ)	s.e.m.	N*
eYFP	268	± 44	16,16,3
iC++	299	± 18	58,58,9

eYFP vs. iC++: P>0.05, t = 0.75;
*N: total number of measurements, cells, number of separately prepared and transfected cell culture batches

Supplementary Table for Supplementary Figure 2D

	V_{AP} (mV)	s.e.m.	V_{Rest} (mV)	s.e.m.	N*
eYFP	-48.0	± 0.7	-58.9	± 2.5	16,16,3
iC++	-50.0	± 0.5	-62.0	± 1.1	58,58,9

V_{AP}: eYFP vs. iC++: P>0.05, t = 1.41, eYFP vs. eNpHR3.0: P>0.05, t = 0.13
V_{Rest}: eYFP vs. iC++: P>0.05, t = 0.36, eYFP vs. eNpHR3.0: P<0.05, t = 2.65
*N: total number of measurements, cells, number of separately prepared and transfected cell culture batches

Supplementary Table for Supplementary Figure 2E

$[HCO^-_3]_{ext}$	V_{rev}	s.e.m.	N*
0 mM	-53.5	± 2.2	13,13,3
26 mM	-52.2	± 1.9	11,11,2

0 mM vs. 26 mM: P>0.05, t = 0.64
*N: total number of measurements, cells, number of separately prepared and transfected cell culture batches

Supplementary Table for Supplementary Figure 2H

$[Aspartate^-]_{int}$ 140 mM $[X^-]_{ext}$ 140 mM	V_{rev} (mV)	s.e.m.	N*
Aspartate	-3.6	± 0.5	11,11,2
Gluconate	-6.0	± 1.4	5,5,1
Chloride	-65.7	± 1.3	6,6,1
Bromide	-76.1	± 0.8	6,6,1
Iodide	-76.7	± 1.0	8,8,1

*N: total number of measurements, cells, number of separately prepared and transfected cell culture batches

Supplementary Table for Supplementary Figure 3A

	V_{Rest} (mV)	s.e.m.	N*
eYFP	-78.2	± 2.1	21,21,2
iC++	-77.3	± 1.1	61,61,7

V_{Rest}: eYFP vs. iC++: P>0.05, t = 0.37,
*N: total number of measurements, cells and animals used for slice electrophysiology

Supplementary Table for Supplementary Figure 3B

	R_{in} (MΩ)	s.e.m.	N*
eYFP	186	± 16	22,22,2
iC++	189	± 13	89,89,10

eYFP vs. iC++: P>0.05, t = 0.12
*N: total number of measurements, cells and animals used for slice electrophysiology

Supplementary Table for Supplementary Figure 3D

$[Cl^-]_{ext}$ 132 mM	30 ms AP Inh. prob.	s.e.m.	Median	Q1	N	5 ms AP Inh. prob.	s.e.m.	Median	Q1	N*
$[Cl^-]_{int}$ 4 mM	0.89	± 0.07	1	0.85	9,9,3	0.71	± 0.13	1	0.62	18,18,2
$[Cl^-]_{int}$ 12 mM	1	± 0	1	1	9,9,4	0.34	± 0.15	0.085	0	18,18,3
$[Cl^-]_{int}$ 20 mM	0.78	± 0.08	0.99	0.63	14,14,5	0.23	± 0.17	0.02	0	8,8,3

30 ms: 4 mM vs. 12 mM inhibition probability: P>0.05, t = 0.91, 4 mM vs. 20 mM: P>0.05, t = -1.1, 12 mM vs. 20 mM: P>0.05, t = -2.1
5 ms: 4 mM vs. 12 mM inhibition probability: P<0.005, t = -3.44, 4 mM vs. 20 mM: P<0.005, t = -3.37, 12 mM vs. 20 mM: P>0.05, t = -0.68
*N: total number of measurements, cells and animals used for slice electrophysiology

Supplementary Table for Supplementary Figure 3E

	R_{in} (MΩ)	s.e.m.	N*
eYFP	186	± 16	22,22,2
iC++	189	± 13	89,89,10
eNpHR3.0	182	± 13	26,26,3

eYFP vs. iC++: P>0.05, t = 0.12, eYFP vs. eNpHR3.0: P>0.05, t = 0.19
*N: total number of measurements, cells and animals used for slice electrophysiology

Supplementary Table for Supplementary Figure 3F

	V_{AP} (mV)	s.e.m.	V_{Rest} (mV)	s.e.m.	N*
eYFP	-57.2	± 0.6	-78.2	± 2.1	21,21,2
iC++	-53.9	± 0.5	-77.3	± 1.1	61,61,7
eNpHR3.0	-59.3	± 0.6	-71.1	± 1.6	26,26,3

V_{AP}: eYFP vs. iC++: P<0.0001, t = 4.24, eYFP vs. eNpHR3.0: P<0.05, t = 2.52
V_{Rest}: eYFP vs. iC++: P>0.05, t = 0.37, eYFP vs. eNpHR3.0: P<0.05, t = 2.7
*N: total number of measurements, cells and animals used for slice electrophysiology

Supplementary Table for Supplementary Figure 4A, B

$[Cl^-]_{ext}$ 147 mM $[Cl^-]_{int}$ 12 mM	V_{rev} (mV)	s.e.m.	PC at V_{AP} (pA)	s.e.m.	N*
iC1C2	-56	± 2	18	± 3	15,15,4
SwiChR_CA	-55	± 2	21	± 3	15,15,3
iC++	-67	± 1	164	± 16	25,25,5
SwiChR++	-66	± 1	111	± 12	17,17,5

N: total number of measurements, cells, number of separately prepared and transfected cell culture batches

Supplementary Table for Supplementary Figure 4C

$[Cl^-]_{ext}$ 147 mM $[Cl^-]_{int}$ 12 mM	30 ms AP Inh. prob.	s.e.m.	Median	Q1	N*
iC1C2	0.11	± 0.03	0.03	0	14,14,4
SwiChR_CA	0.41	± 0.11	0.3	0	13,13,3
iC++	0.91	± 0.06	1	0.75	7,7,2
SwiChR++	1	± 0	1	1	7,7,2

AP inhibition probability: iC1C2 vs. iC++: P<0.0001, U = 0, SwiChR_CA vs. SwiChR++: P<0.005, U = 84
N: total number of measurements, cells, number of separately prepared and transfected cell culture batches

Supplementary Table for Supplementary Figure 4C

$[Cl^-]_{ext}$ 147 mM $[Cl^-]_{int}$ 12 mM	5 ms AP Inh. prob.	s.e.m.	Median	Q1	N*
iC1C2	0	± 0	0	0	8,8,2
SwiChR_CA	0.02	± 0.02	0	0	8,8,1
iC++	0.89	± 0.07	1	1	17,17,5
SwiChR++	0.74	± 0.11	1	0.35	15,15,5

iC1C2 vs. iC++ AP inhibition probability: P<0.005, U = 12, SwiChR_CA vs. SwiChR++: P<0.005, U = 13.5
N: total number of measurements, cells, number of separately prepared and transfected cell culture batches

Supplementary Table for Supplementary Figure 4E

	Input resistance (MΩ)	s.e.m.	V_{Rest} (mV)	s.e.m.	N*
eYFP	268	± 44	-59	± 3	16,16,3
SwiChR++	231	± 29	-62	± 2	14,14,5

Input resistance: P>0.05, t = 0.68; V_{Rest}: P>0.05, t = 1.07
N: total number of measurements, cells, number of separately prepared and transfected cell culture batches

Supplementary Table for Supplementary Figure 4F

	Input resistance (MΩ)	s.e.m.	V_{Rest} (mV)	s.e.m.	N*
eYFP	186	± 16	-78	± 2	22,22,2
SwiChR++	182	± 14	-76	± 1	31,31,6

Input resistance: P>0.05, t = 0.18; V_{Rest}: P>0.05, t = 0.98
*N: total number of measurements, cells and animals used for slice electrophysiology

Supplementary Table for Supplementary Figure 4H

$[Cl^-]_{ext}$ 132 mM	30 ms AP Inh. prob.	s.e.m.	Median	Q1	N*
$[Cl^-]_{int}$ 4 mM	0.87	± 0.13	1	0.99	8,8,3
$[Cl^-]_{int}$ 12 mM	0.87	± 0.1	0.96	0.91	15,15,4
$[Cl^-]_{int}$ 20 mM	0.45	± 0.1	0.39	0.08	15,15,4

30 ms: 4 mM vs. 12 mM inhibition probability: P>0.05, t = -0.01, 4 mM vs. 20 mM: P<0.05, t = -2.93, 12 mM vs. 20 mM: P<0.005, t = -3.5
*N: total number of measurements, cells and animals used for slice electrophysiology

Supplementary Table for Supplementary Figure 4H

$[Cl^-]_{ext}$ 132 mM	5 ms AP Inh. prob.	s.e.m.	Median	Q1	N*
$[Cl^-]_{int}$ 4 mM	0.47	± 0.12	0.37	0.125	12,12,3
$[Cl^-]_{int}$ 12 mM	0.08	± 0.05	0	0	7,7,2
$[Cl^-]_{int}$ 20 mM	0	±0	0	0	6,6,2

5 ms: 4 mM vs. 12 mM inhibition probability: P<0.05, t = -2.85, 4 mM vs. 20 mM: P<0.05, t = -3.27, 12 mM vs. 20 mM: P>0.05, t = -0.5
*N: total number of measurements, cells and animals used for slice electrophysiology

Supplementary Table for Supplementary Figure 5F

$[Cl^-]_{ext}$ 132 mM	pre light AP frequency (Hz)	s.e.m.	light AP frequency (Hz)	s.e.m.	post light AP frequency (Hz)	s.e.m.	N*
cell #1	22.2	± 2.4	4.9	± 1.7	9.8	± 2.2	15
cell #2	33.9	± 5.2	8.1	± 3.0	19.3	± 6.8	13
cell #3	5.7	± 0.8	4.9	± 0.6	5.7	± 0.6	15

cell #1, ANOVA: P<0.001, $F_{2, 42}$ = 17.63
cell #2, ANOVA: P<0.01, $F_{2, 36}$ = 6.15
cell #3, ANOVA: P>0.05, $F_{2, 42}$ = 0.52
*N: total number of trials

Supplementary Table for Supplementary Figure 6C

$[Cl^-]_{ext}$ 132 mM	5 ms AP Inh. prob.	s.e.m.	Median	Q1	N*
$[Cl^-]_{int}$ 4 mM	0.76	± 0.1	1	0.63	16,16,2
$[Cl^-]_{int}$ 12 mM	0.86	± 0.06	0.92	0.68	8,8,2
$[Cl^-]_{int}$ 20 mM	0.32	± 0.16	0.03	0	8,8,3

Inhibition probability: 4 mM vs. 12 mM: P>0.05, t = 0.56, 4 mM vs. 20 mM: P<0.05, t = -2.81, 12 mM vs. 20 mM: P<0.05, t = -2.93
*N: total number of measurements, cells and animals used for slice electrophysiology

Supplementary Table for Supplementary Figure 6E, F, G

$[Cl^-]_{ext}$ 132 mM $[Cl^-]_{int}$ 4 mM	pre TGOT V_m (mV)	s.e.m.	TGOT V_m (mV)	s.e.m.	post TGOT V_m (mV)	s.e.m.	N	V_m change peak (ΔmV)	s.e.m.	V_m change stst (ΔmV)	s.e.m.	N*
iC++ in HC-PV+	-75.7	1.6	-64.7	1.8	-72.6	2.2	7	-12.0	1.1	-3.5	1.8	6,6,2

V_m: pre vs. TGOT inhibition: P<0.005, t = 4.21, pre vs. post TGOT: P>0.05, t = 1.19, post vs. TGOT: P<0.05, t = -3.01
*N: total number of measurements, cells and animals used for slice electrophysiology

Supplementary Table for Supplementary Figure 6H,

mM: $[Cl^-]_{ext}$ 132 $[Cl^-]_{int}$ 12	10 ms AP Inh. prob.	s.e.m.	Median	Q1	N*
mPFC-pyr	0.69	± 0.09	1	0	27,27,6
HC-PV	0.98	± 0.02	1	1	8,8,3
SN-dop	0.97	± 0.02	1	1	15,15,4
DRG	1	± 0	1	1	14,14,1

AP inhibition probability: mPFC, HC-PV: P<0.005, t = 3.38, mPFC, SN-dop: P<0.005, t = 3.18, mPFC, DRG: P<0.005, t = 3.62
*N: total number of measurements, cells and animals used for slice electrophysiology

Supplementary Table for Supplementary Figure 6I, J, K, L, M

mM: $[Cl^-]_{ext}$ 132 $[Cl^-]_{int}$ 12	PC at V_{AP} (pA)	s.e.m.	Curr. inject. (pA)	s.e.m.	V_{AP} (mV)	s.e.m.	V_{Rest} (mV)	s.e.m.	Cell capac. (pF)	s.e.m.	R_{in} (MΩ)	s.e.m.	N*
mPFC-pyr	179	± 25	427	± 34	-53	± 1	-79	± 2	88	± 6	197	25	27,27,6
HC-PV	194	± 40	360	± 48	-55	± 2	-74	± 1	70	± 6	110	11	8,8,3
SN-dop	185	± 27	342	± 39	-47	± 1	-57	± 2	54	± 5	473	79	15,15,4
DRG	288	± 63	241	± 27	-33	± 1	-59	± 1	25	± 2	445	73	14,14,1

PC at V_{AP}: mPFC, HC-PV: P>0.05, t = 0.31, mPFC, SN-dop P>0.05 t = 0.16, mPFC, DRG: P>0.05, t = 1.63
Current injection: mPFC, HC-PV: P>0.05, t = 0.98, mPFC, SN-dop P>0.05 t = 1.57, mPFC, DRG: P<0.005, t = 4.27
V_{AP}: mPFC, HC-PV: P>0.05, t = 0.66, mPFC, SN-dop P<0.005 t = 4.23, mPFC, DRG: P<0.0001, t = 13.49
V_{Rest}: mPFC, HC-PV: P>0.05, t = 2.53, mPFC, SN-dop P<0.0001 t = 7.52, mPFC, DRG: P<0.0001, t = 7.26
Capacitance: mPFC, HC-PV: P<0.05, t = 2.81, mPFC, SN-dop P<0.005 t = 4.42, mPFC, DRG: P<0.0001, t = 10.38
R_{in}: mPFC, HC-PV: P<0.005, t = 3.23, mPFC, SN-dop P<0.005 t = 3.37, mPFC, DRG: P<0.01, t = 3.19
*N: total number of measurements, cells and animals used for slice electrophysiology

Supplementary Table for Supplementary Figure 7C

$[Cl^-]_{ext}$ 132 mM $[Cl^-]_{int}$ 4 mM	Hyperpolarization from V_{AP} (@ Min. AP thresh.) (ΔmV)	s.e.m.	Hyperpolarization from V_{AP} (@ Max. current w/o spikes) (ΔmV)	s.e.m.	N*
iC++	-6.6	± 1.2	n.A.	n.A.	12,12,3
eNpHR3.0	-41.4	± 6.3	-7.7	± 1.1	12,12,3

*N: total number of measurements, cells and animals used for slice electrophysiology

Supplementary Table for Supplementary Figure 7D

$[Cl^-]_{ext}$ 132 mM $[Cl^-]_{int}$ 4 mM	Min for AP threshold (pA)	s.e.m.	Max w/o spikes (light on) (pA)	s.e.m.
iC++	131	± 25	2098	± 267
eNpHR3.0	75	± 9	444	± 85

Max. inhibited: iC++(4) vs. eNpHR3.0: P<0.005, t = 5.02,
*N: total number of measurements, cells and animals used for slice electrophysiology

Supplementary Table for Supplementary Figure 7E

$[Cl^-]_{ext}$ 132 mM $[Cl^-]_{int}$ 4 mM	Cells w/o spike generation under light (%).	s.e.m.	Median	Q1	N*
iC++	92	± 7	1	1	12,12,3
eNpHR3.0	0	± 0	0	0	12,12,3

*N: total number of measurements, cells and animals used for slice electrophysiology

Supplementary Table for Supplementary Figure 7G,H

$[Cl^-]_{ext}$ 132 mM $[Cl^-]_{int}$ 4 mM	Reduction of R_{in} under light (%)	s.e.m.	Change of membrane potential per current injection (light off) (mV/pA)	s.e.m.	Change of membrane potential per current injection (light on) (mV/pA)	s.e.m.	N*
iC++	79	± 2	0.29	± 0.06	0.04	± 0.01	12,12,3
eNpHR3.0	39	± 4	0.23	± 0.03	0.12	± 0.02	12,12,3

PC: iC+ vs. eNpHR3.0: P>0.05, t = 1.76
Reduction of R_{in}: iC++ vs. eNpHR3.0: P<0.0001, t = 9.67
Change of membrane potential (light): iC++ vs. eNpHR3.0: P<0.005, t = 3.37
*N: total number of measurements, cells and animals used for slice electrophysiology

Supplementary Table for Supplementary Figure 7I

$[Cl^-]_{ext}$ 132 mM $[Cl^-]_{int}$ 4 mM	10 ms current injection (Min) (pA)	s.e.m.	10 ms current injection (Max) (pA)	s.e.m.	N*
iC++	459	± 94	1357	± 268	11,11,3
eNpHR3.0	348	± 46	711	± 97	11,11,3

Max. inhibited: iC++(4) vs. eNpHR3.0: P<0.05, t = 2.13
*N: total number of measurements, cells and animals used for slice electrophysiology

Supplementary References:

1. Berndt A, Lee SY, Ramakrishnan C, & Deisseroth K (2014) Structure-guided transformation of channelrhodopsin into a light-activated chloride channel. *Science* 344(6182):420-424.
2. Gradinaru V, *et al.* (2010) Molecular and cellular approaches for diversifying and extending optogenetics. *Cell* 141(1):154-165.
3. Baker NA, Sept D, Joseph S, Holst MJ, & McCammon JA (2001) Electrostatics of nanosystems: application to microtubules and the ribosome. *Proc Natl Acad Sci U S A* 98(18):10037-10041.
4. Iyer SM, *et al.* (2014) Virally mediated optogenetic excitation and inhibition of pain in freely moving nontransgenic mice. *Nat Biotechnol* 32(3):274-278.
5. Hippenmeyer S, *et al.* (2005) A developmental switch in the response of DRG neurons to ETS transcription factor signaling. *PLoS Biol* 3(5):e159.
6. Zhuang X, Masson J, Gingrich JA, Rayport S, & Hen R (2005) Targeted gene expression in dopamine and serotonin neurons of the mouse brain. *J Neurosci Methods* 143(1):27-32.
7. Wietek J, *et al.* (2014) Conversion of channelrhodopsin into a light-gated chloride channel. *Science* 344(6182):409-412.
8. Schmitzer-Torbert N, Jackson J, Henze D, Harris K, & Redish AD (2005) Quantitative measures of cluster quality for use in extracellular recordings. *Neuroscience* 131(1):1-11.
9. Backman CM, *et al.* (2006) Characterization of a mouse strain expressing Cre recombinase from the 3' untranslated region of the dopamine transporter locus. *Genesis* 44(8):383-390.
10. Cole CJ, *et al.* (2012) MEF2 negatively regulates learning-induced structural plasticity and memory formation. *Nat Neurosci* 15(9):1255-1264.
11. Hsiang HL, *et al.* (2014) Manipulating a "cocaine engram" in mice. *J Neurosci* 34(42):14115-14127.
12. Josselyn SA, *et al.* (2001) Long-term memory is facilitated by cAMP response element-binding protein overexpression in the amygdala. *J Neurosci* 21(7):2404-2412.
13. Vetere G, *et al.* (2011) Spine growth in the anterior cingulate cortex is necessary for the consolidation of contextual fear memory. *Proc Natl Acad Sci U S A* 108(20):8456-8460.
14. Yiu AP, *et al.* (2014) Neurons are recruited to a memory trace based on relative neuronal excitability immediately before training. *Neuron* 83(3):722-735.
15. Paxinos G & Franklin KBJ (2001) *The mouse brain in stereotaxic coordinates* (Academic Press, San Diego) 2nd Ed.